

This article was downloaded by:

On: 22 January 2011

Access details: *Access Details: Free Access*

Publisher *Taylor & Francis*

Informa Ltd Registered in England and Wales Registered Number: 1072954 Registered office: Mortimer House, 37-41 Mortimer Street, London W1T 3JH, UK



The Journal of Adhesion

Publication details, including instructions for authors and subscription information:

<http://www.informaworld.com/smpp/title~content=t713453635>

Viscoelastic and Processing Effects on the Fiber-Matrix Interphase Strength. Part III. The Effects of Postcure

Erol Sancaktar^a; Weijian^a

^a Department of Mechanical and Aeronautical Engineering, Clarkson University, Potsdam, New York, U.S.A.

To cite this Article Sancaktar, Erol and Weijian(1992) 'Viscoelastic and Processing Effects on the Fiber-Matrix Interphase Strength. Part III. The Effects of Postcure', *The Journal of Adhesion*, 38: 1, 131 – 151

To link to this Article: DOI: 10.1080/00218469208031271

URL: <http://dx.doi.org/10.1080/00218469208031271>

PLEASE SCROLL DOWN FOR ARTICLE

Full terms and conditions of use: <http://www.informaworld.com/terms-and-conditions-of-access.pdf>

This article may be used for research, teaching and private study purposes. Any substantial or systematic reproduction, re-distribution, re-selling, loan or sub-licensing, systematic supply or distribution in any form to anyone is expressly forbidden.

The publisher does not give any warranty express or implied or make any representation that the contents will be complete or accurate or up to date. The accuracy of any instructions, formulae and drug doses should be independently verified with primary sources. The publisher shall not be liable for any loss, actions, claims, proceedings, demand or costs or damages whatsoever or howsoever caused arising directly or indirectly in connection with or arising out of the use of this material.

J. Adhesion, 1992, Vol. 38, pp. 131–151
Reprints available directly from the publisher
Photocopying permitted by license only
© 1992 Gordon and Breach Science Publishers S.A.
Printed in the United Kingdom

Viscoelastic and Processing Effects on the Fiber-Matrix Interphase Strength. Part III. The Effects of Postcure*

EROL SANCAKTAR and WEIJIAN MA

Department of Mechanical and Aeronautical Engineering, Clarkson University, Potsdam, New York 13699-5725, U.S.A.

(Received April 25, 1991; in final form January 13, 1992)

A novel method for tailoring the interphase of carbon fiber-polymer composites by resistive electric heating is presented. The single-fiber fragmentation test is used to investigate the adhesion and fracture properties of the interphase. Electric resistive heating is shown to increase adhesion and toughness at the interphase region. In analyzing the results, the strength and fracture energy of the interphase are related to the thermal postcure conditions created by resistive electric heating. For this purpose, a difference analysis method is used to obtain a numerical solution for the heat conduction problem in the single-fiber test specimen and the temperature distributions are determined. Improvements obtained by using resistive electric heating of the carbon fiber are compared with those obtained by postcuring of the whole sample *via* convective thermal postcuring. The results obtained using these two different postcure methods seem to be similar.

KEY WORDS Fiber-matrix interphase; resistive electric heat postcure; convective thermal heat postcure; fiber-matrix adhesion; fiber-end cracking.

INTRODUCTION

Improvement of the mechanical behavior of composites by improving the performance of their individual components and their interaction has been an important aspect of composites research. The fiber-matrix interphase is the focus of recent research since abrupt changes of stress fields occur there. The investigation presented here proposes to tailor the interphase in carbon fiber-epoxy composites by resistive electric heating of carbon fibers. During this tailoring process the conducting carbon fiber produces a thermal field and is expected to cause favorable elastic modulus, toughness and/or strength distribution in the matrix around it, thus forming a mechanically-superior interphase with less residual stress. Agrawal and

*Presented in part at the 14th Annual Meeting of The Adhesion Society, Inc., Clearwater, Florida, U.S.A., February 17–20, 1991.

Drzal¹ recently reported that during microwave curing of carbon-epoxy composites “the conductive carbon fiber absorbed a large portion of the electromagnetic radiation and produced interfacial strengths higher than that achievable in thermally cured systems.”

The majority of graphite-epoxy composite failures occur due to catastrophic crack propagations. Consequently, it is very desirable to reduce the possibility of any crack formation in composite materials. A recent work by Sancaktar and Zhang² showed that global loading of composite materials resulting in fiber breakage also leads to high stress concentrations near the fiber ends. Microscopic examination of such fiber-end regions in single-fiber fragmentation test specimens revealed the presence of matrix cracks. The main objective of the current work is to reduce the number and size of such cracks and, hence, to reduce the possibility of catastrophic failure in graphite-epoxy composite systems.

High temperature curing has been shown to increase deformability and toughness of epoxy adhesives.^{3,4,5} If the deformability and the thickness of the fiber-matrix interphase can be increased by electric heating through the fiber, then the shear stress peaks which exist near the fiber ends are reduced, thus distributing the shear stress more uniformly and efficiently along the fiber. This behavior has recently been shown analytically for a nonlinear viscoelastic interphase and matrix by Sancaktar and Zhang.²

Elementary fracture mechanics theory⁶⁻⁸ dictates that longer and a larger number of cracks are formed when the toughness of a material is low. An approximate but simple way to measure the toughness of a material is to calculate the approximate elastic energy it will store up to yield, σ_y , by simply dividing the σ_y^2 by its elastic modulus, E . Higher σ_y^2/E values indicate higher toughness and, consequently, less

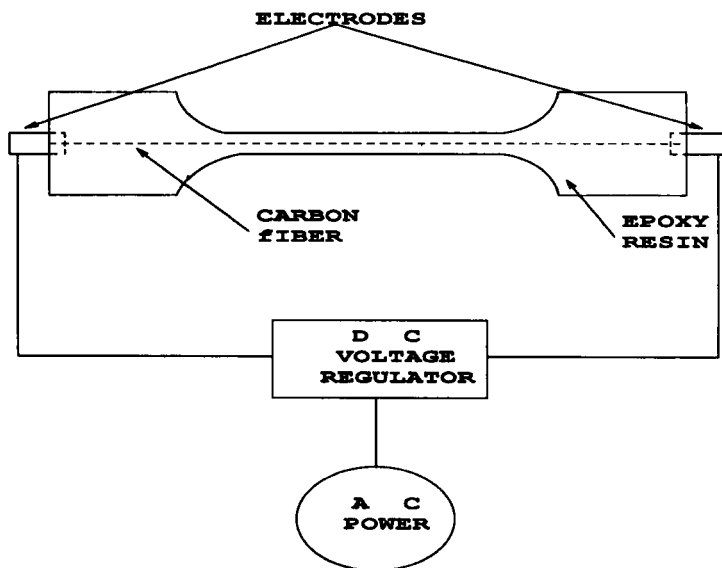


FIGURE 1 Resistive Electric Heating Circuit Diagram.

likelihood for crack formation and propagation. On this basis, processing conditions which will result in higher yield stress and lower modulus will provide tougher composites. Previous work on epoxy cure optimization, however, showed that most cure and postcure conditions used to increase polymer strength also increase the polymer's elastic modulus.^{3,4} On the other hand, an increase in the polymer's elastic modulus does not necessarily result in a decrease in its toughness, due to the higher order dependence of toughness on stress (σ_y^2) and also due to the difference in the relative increase in σ_y and E .

In this investigation, a set of experiments has been performed to find the effects of conducting electric current through the embedded carbon fibers on the material properties and failure behavior of the epoxy matrix around it. The experiments were performed using the single-fiber fragmentation test.⁹⁻¹¹ Consequently, the number and sizes of the fiber fragments and cracks in the matrix interphase were measured to assess the effects of electric heating. In order to understand the processing effect of resistive electric heating, a group of specimens were treated by thermal postcure without resistive electric heating and subsequently tested using the single fiber fragmentation test procedure to find the differences between electric heating and thermal heating postcures.

The circuit diagram of resistive electric heating is shown in Figure 1.

THEORETICAL CONSIDERATIONS

Material and Cure Considerations

The interphase formed between the carbon fibers and epoxy resin matrix serves two important purposes: transferring load to carbon fibers and preventing failure propagation. The adhesion between the fiber and the matrix and the toughness of the interphase determine how well these purposes are served.

Some basic knowledge of epoxy resin chemistry and properties is needed for understanding the interphase phenomenon.^{12,13}

Epoxy resins are rigid, amorphous, glasslike solids. Theories, and evidence based on electron microscopy, suggest that cured epoxy resins have many relatively small three-dimensional branches forming a network of moderate molecular weight material. Due to steric hindrance that minimizes intermolecular reactions, the final size of network during cure is limited. When the molecules polymerize, their rotational and translational freedom is reduced, which reduces the chances for primary bonds to be set up with adjacent molecules.

When the epoxy resin is subjected to postcure at elevated temperatures, the increased thermal agitation permits an additional number of sterically-hindered epoxy groups to react. Thus, the size of the crosslink network is increased at the expense of the surrounding lower molecular weight material, which has lower strength, lower hardness and lower solvent resistance than the highly cross-linked network. In general, irrespective of the curing agent, postcuring at temperatures higher than the initial cure temperature will produce improvements.¹²⁻¹⁵ It should be noted, however, that mechanical properties of thermosetting polymers can only be improved up to a limit with increasing cure temperature and time values. Further

increases in cure (and postcure) temperature and time values usually result in deterioration of mechanical properties. For example, the yield strength and the elastic modulus when plotted against the cure temperature behaves as a bell-shaped function: first it increases up to a limit and then decreases³⁻⁵ at elevated temperature postcure. Postcuring at too high temperatures and long time periods also results in a reduction of the fracture energy.^{4,16}

Interfacial Shear Stress

Interfacial shear stress between a carbon fiber and an epoxy matrix is related to the adhesion phenomenon. Dara and Loos^{17,18} proposed the following relation for the adhesion strength σ_{ad} :

$$\sigma_{ad} = e(a_t t_{c,ref})^b \quad (1)$$

In equation (1) e and b are constants, a_t is the WLF shift factor, and $t_{c,ref}$ is the contact time. The shift factor a_t is defined by the relation

$$\log a_t = -a_1(T - T_{ref}) / \{a_2 + (T - T_{ref})\} \quad (2)$$

where a_1 and a_2 are constants, T is the temperature and T_{ref} is the reference temperature. Consequently, equation (1) dictates that the equivalent contact time at temperatures other than a reference temperature (such as the glass transition temperature T_g) is defined by equation

$$t_c = a_t t_{c,ref} \quad (3)$$

Elevated postcure temperature increases the mobility of polymer molecules, therefore promoting diffusion and, hence, adhesion.

Many researchers use single fiber-resin tensile tests to determine the adhesion between fiber and resin. Assuming uniform fiber strength and diameter, Kelly^{19,20} derived an expression for this adhesion strength (τ_c) in the form

$$\tau_c = (\sigma_f d) / (2 l_c) \quad (4)$$

where τ_c is the shear strength at the fiber resin interface, d is the fiber diameter, l_c is the critical fiber fragment size and σ_f is the fiber tensile strength. As described by Kelley, when a tensile load is applied to the fiber-matrix composite, the fiber should break into fragments until an l_c is reached which is too short to transfer stress equal or greater than σ_f . The l_c is believed to indicate the shear strength of fiber-matrix adhesion. In other words, shorter l_c means larger shear stress τ_c which shows better adhesion.

Fracture Considerations

The Irwin criterion for fracture is based on equating the strain energy with the crack surface energy at the instant of crack propagation. Such an energy balance results in the equation

$$\sigma_c^2 = (EG_c) / (\pi a) \quad (5)$$

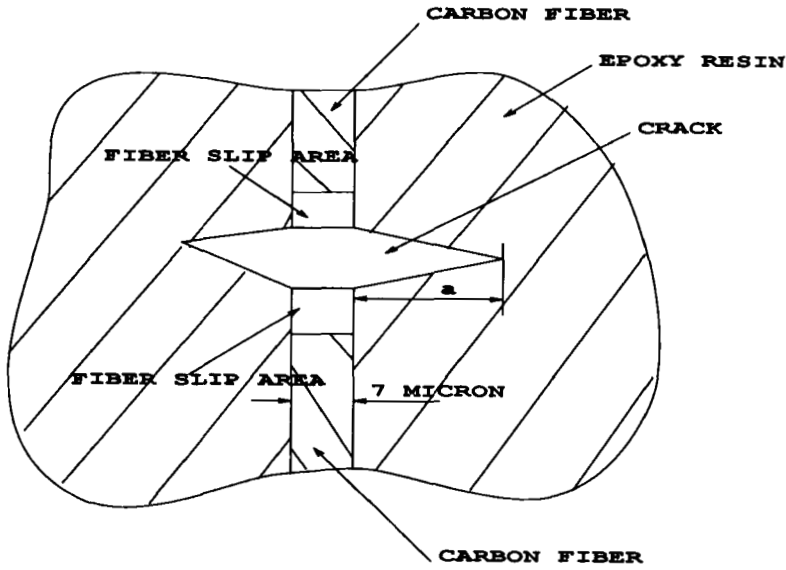


FIGURE 2 The Geometry of the Break and Crack in Tested Specimen.

where G_c , being an index of fracture toughness, is the strain energy release rate (related to fracture energy), E is the elastic modulus, σ_c is the stress at crack initiation, and a is one-half of the initial crack length (See Figure 2).

Equation (5) can be rewritten as

$$G_c = \sigma_c^2 \pi a / E \quad (6)$$

Obviously, if a is constant, then σ_c^2/E can be used as an index of G_c . This approach allows the number of cracks within a length category (such as $5\mu\text{m} < a < 20\mu\text{m}$, see Table IV) to be compared as a function of different processing conditions (*i.e.* electric postcure, etc.). Note that higher G_c means higher toughness²¹⁻²⁵ and, consequently, cracks are unlikely to propagate easily in high G_c regions.

Thermal Considerations

This investigation deals with affecting the interphase between the carbon fiber and the epoxy matrix by producing a high temperature gradient around the fiber. Electric resistive heating is used for this purpose. The interphase near the fiber could develop higher strength due to the postcure effects derived from high temperatures. Consequently, stronger adhesion and better resistance to crack propagation are expected.

The thermal fields produced by electric resistive heating of carbon fibers are different from those produced by the thermal heating originally used to cure the matrix. The temperature distribution around the fiber and in the interphase is needed for considering the effects of electric heating on the carbon fiber/epoxy resin interphase.

The Heat Transfer Problem

In our experiments, the surfaces of the specimens had an assumed constant room temperature of 25°C due to their rather large surface area, small heat output and good heat convection to the ambient air. Therefore, a purely heat conduction problem can be assumed for the specimens. The general governing equation for heat conduction is

$$(\partial T / \partial t) = a \nabla^2 T + p(x, y, z). \quad (7)$$

For this first research stage, only the temperature distribution on one resin cross-section was calculated, thus reducing the problem to a 2-dimensional one. Furthermore, the temperature distribution does not change with time after thermal equilibrium is established, and consequently, it is a steady temperature condition.

Based on these assumptions, the 2-dimensional heat transfer equation (7) is reduced to a Poisson equation

$$(\partial^2 T / \partial x^2) + (\partial^2 T / \partial y^2) = f(x, y). \quad (8)$$

The geometry of the specimens is shown in Figure 3. Except for the carbon fiber cross-section, which is the heat source (point C in Figure 4), there is no other heat source or sink. This means that in equation (8) $f(x, y) = 0$, except for point C. As a result, equation (8) can be reduced to Laplace equation

$$(\partial^2 T / \partial x^2) + (\partial^2 T / \partial y^2) = 0. \quad (9)$$

Methods of numerical analysis need to be used to solve the Laplace equation. Here, a difference analysis method is used to obtain a numerical solution. The corresponding difference equation is

$$T(x, y) = [T(x + \Delta x, y) + T(x - \Delta x, y) + T(x, y + \Delta y) + T(x, y - \Delta y)] / 4 \quad (10)$$

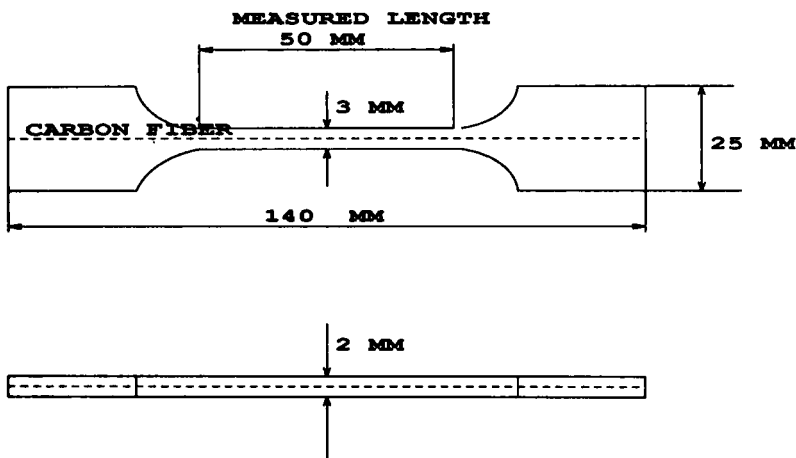


FIGURE 3 The Geometry of the Specimen.

The specimen cross-sections were divided into a 12×8 grid with $\Delta x = 0.25$ mm and $\Delta y = 0.25$ mm (See Figure 4). Due to the geometric symmetry of the cross-section, the unknown variables are reduced to 23. T_1, T_2, \dots, T_{23} are temperatures at points 1, 2, ..., 23. T_c is the temperature at point C. Thus equation (10) becomes a set of 23 linear equations containing 24 unknowns. There are two boundaries, the outer surface of the specimen and the carbon fiber surface. On the specimen's outer surface, the temperature $T_o = 25^\circ\text{C}$. The temperature T_c , however, needs to be calculated. The energy balance principle requires that the amount of electric heat produced in the carbon fiber should be equal to the amount of heat transferred from the specimen surface to the ambient air under steady-state conditions. Furthermore, it is assumed that the heat transfers perpendicularly from the carbon fiber surface through the specimen surface to still air. Thus an additional equation is established

$$Q = \lambda u \Sigma \Delta T_{av,s} \tag{11}$$

where u is a chosen length along the fiber axis, Q is the electric energy per second produced in a fiber having length u , λ is the thermal conductivity of the epoxy resin and $\Sigma \Delta T_{av,s}$ is the sum of the average temperature differences perpendicular to the surface of the specimen for each grid contacting air, that is

$$\Sigma \Delta T_{av,s} = 2[50 + T_1 + T_{23} + 2(2T_6 + T_{12} + T_{18} + T_5 + T_4 + T_3 + T_2)] - 40 \times 25 \tag{12}$$

In our calculation:

$$\lambda = 2.1 \times 10^{-3} \text{ J/cm} \cdot ^\circ\text{C} \cdot \text{s}$$

$$Q_{I=3.5\text{mA}} = 0.0573 \text{ J/s}$$

$$Q_{I=5.0\text{mA}} = 0.117 \text{ J/s}$$

$$Q_{I=6.5\text{mA}} = 0.198 \text{ J/s}$$

$$U = 10 \text{ mm.}$$

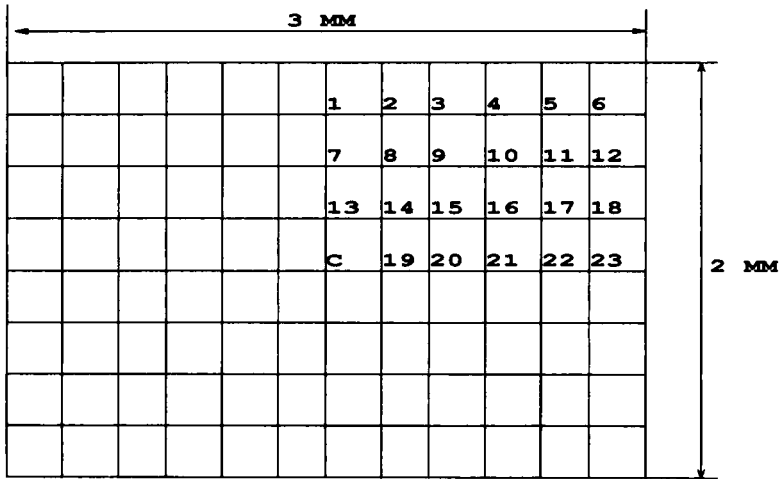


FIGURE 4 The Cross-section of the Specimen and Grid for Temperature Calculation.

Downloaded At: 14:08 22 January 2011

The Inverse Matrix Method²⁶ is used to solve the equations (10) with the aid of a computer program prepared for this purpose. The calculated results are shown in Figures 5–7. As can be seen, for a carbon current $I=3.5$ mA, the carbon surface temperature was $T_c=38.67^\circ\text{C}$, for $I=5.0$ mA, $T_c=52.34^\circ\text{C}$, and for $I=6.5$ mA, $T_c=74.22^\circ\text{C}$. The results reveal that the temperature gradients around the carbon fiber increase as the current is increased.

It should be noted that the difference equation method and inverse matrix method can also be used to solve the three-dimensional Poisson equation and the Laplace equation for heat conduction.

EXPERIMENTAL PROCEDURES

Single carbon fiber/epoxy resin dogbone shaped specimens were made from epoxy resin. The epoxy resin used was Shell Epon 815[®] (Shell Chemical), an epichlorohydrin/bisphenol A-type epoxy resin containing a reactive diluent. The curing agents were DETA (Diethylenetriamine) and Armocure 100 (Akzo Chemicals). DETA is a liquid polyamine widely used with epoxy resins for fast cures and room temperature cures, providing good resin properties at room temperature (or below 82°C , the minimum heat distortion temperature reported by the manufacturer). Armocure 100 is an aliphatic polyamine providing tough, flexible, water-resistant and solvent-resistant epoxy resin. The composition of the epoxy matrix was 88 phr

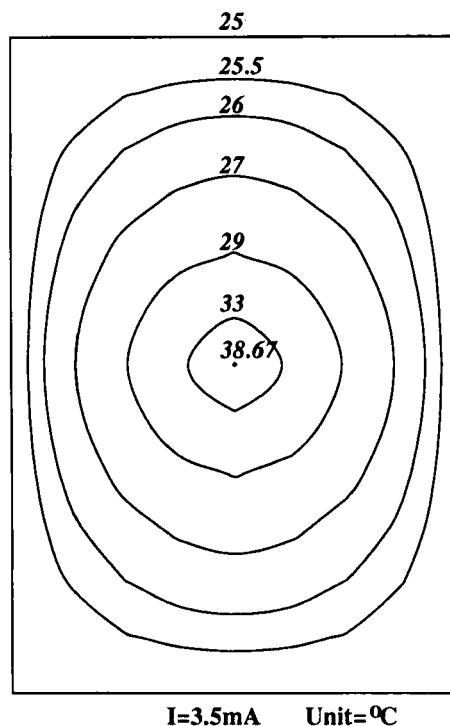
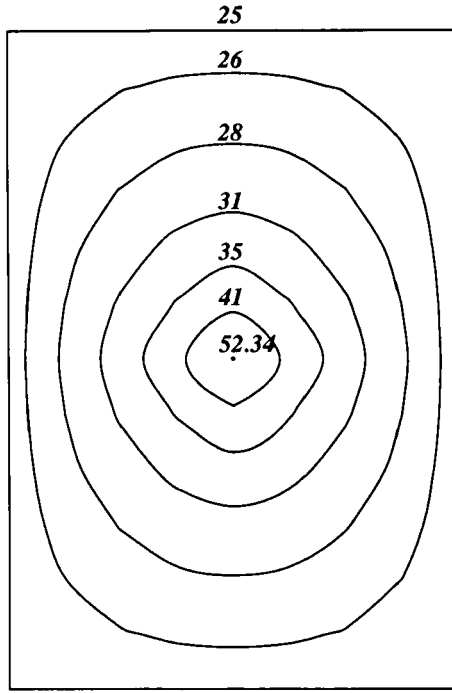
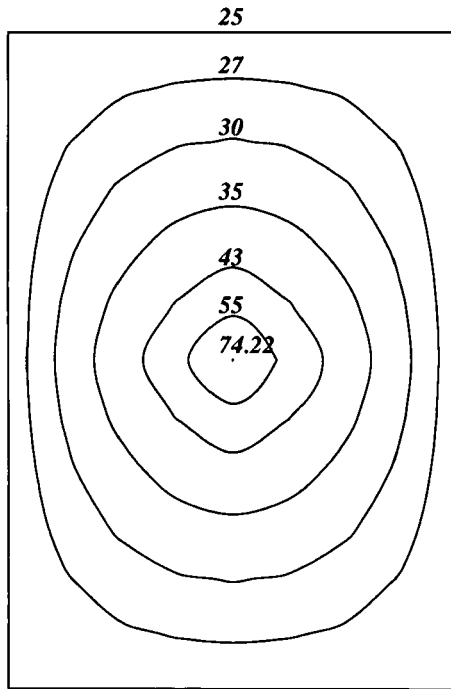


FIGURE 5 The Temperature Distribution on the Cross-section of the Specimen, with $I=3.5$ mA.



I=5.0mA Unit=°C

FIGURE 6 The Temperature Distribution on the Cross-section of the Specimen, with I=5.0 mA.



I=6.5mA Unit=°C

FIGURE 7 The Temperature Distribution on the Cross-section of the Specimen, with I=6.5 mA.

Downloaded At: 14:08 22 January 2011

TABLE I
Electric resistive and thermal postcure conditions

No.	Heating time hour	Carbon current MA	Equiv. postcure temperature °C
0	0	0	25
1	1	3.5	39
2	4	3.5	39
3	8	3.5	39
4	1	5.0	52
5	4	5.0	52
6	8	5.0	52
7	1	6.5	74
8	4	6.5	74
9	8	6.5	74

Note:

No. = postcure condition number

of Epon 815, 12 phr of DETA and 12 phr of Armocure 100. The cure condition was 38°C applied for 12 hours in a convection oven. Several electric and thermal postcures were applied subsequently as the test conditions (See Table I). In order to understand the processing effect of resistive electric heating, a group of specimens were treated by thermal postcure in a convection oven without resistive electric heating. The postcure temperatures applied in this case were matched with the interface temperature created during resistive electric heating. These interface or fiber surface temperatures were calculated using the heat conduction equation as described in a previous section. Hence, they were chosen to be 39°C, 52°C and 74°C, respectively (See Figures 5-7).

The carbon fiber chosen was 7 μm diameter Celion G30 500 (BASF) finished with EP03, an epoxy sizing agent. The electrical resistivity of the carbon fiber was measured and averaged as 0.018 $\Omega\text{-mm}$. In order to apply electric current special electrodes made of aluminum foil were attached on both ends of the fiber using adhesive tape. The fiber was then fixed in an aluminum mold machined specifically to form single-fiber tensile specimens. There was no appreciable change in the circuit resistance subsequent to attachment of aluminum electrodes. The supply voltage was monitored during the electric heat postcure procedure. It was observed that any change in supply voltage was within 5% of the applied value. Care was exercised to prevent contamination of the fibers. After the resin was poured into the molds, vacuum devices were used to remove air from the molded resin. The molds were then put in a convection oven for curing. After curing, the specimens were removed from the molds and machined to the required shape. The electric equipment used for resistive electric postcuring of the specimens was a Regulated Power Supply, Model 50 (Lambda Electronics Corp.) capable of 500 volts maximum DC at 500 milliamperes maximum.

The tensile test machine for the fragmentation tests was a Model 1000 Instron Universal Testing Instrument. Strains were measured using a 4300 Plastics Testing Extensometer with a LVDT Controller. A 7000A/7001A X-Y Recorder was used to plot the stress-strain curves.

A test temperature of 54°C was used to ensure sufficient material deformability to reach 12% strain. The use of such elevated temperature prevented brittle failures

and resulted in consistent critical fiber length l_c values. All single fiber specimens for the fragmentation test were tested to 12% strain to ensure fragmentation of the fiber to the critical length. The extension rate was a fairly slow 3.2 mm/min to (again) avoid premature brittle failures. Excessive necking did not take place during loading and the engineering stress-strain diagrams, in general, did not exhibit any appreciable decrease in stress values once the initial maximum stress level was reached. Fragmentation took place throughout the 50 mm gage length of the specimens. Some of the specimens treated with electric heating or thermal postcure were tested to failure to obtain complete stress-strain diagrams and material properties. Most specimens tested to failure reached about 40% strain.

The values of the elastic moduli E for the epoxy resin were calculated by using the following method:

$$E = 5\text{MPa} / (\epsilon_{\sigma=5\text{MPa}} - \epsilon_{\sigma=0\text{MPa}}) \quad (13)$$

since the $\sigma = 5\text{MPa}$ range visibly corresponds to elastic behavior on the stress-strain diagrams.

The number of carbon fiber breaks and the number of epoxy matrix cracks were observed within a 50 mm gage length of the specimen. The observations of numbers of fiber breaks and matrix cracks were done on a Unitron Microscope (No. Bi-12546) using transmitted light. The magnification used was 100. A BH2-MJLT-L-2 Metallurgical Microscope and a Mitsubishi Video Copy Processor were used to observe and take pictures of cracks in each tests specimen and an example is shown in Figure 8.

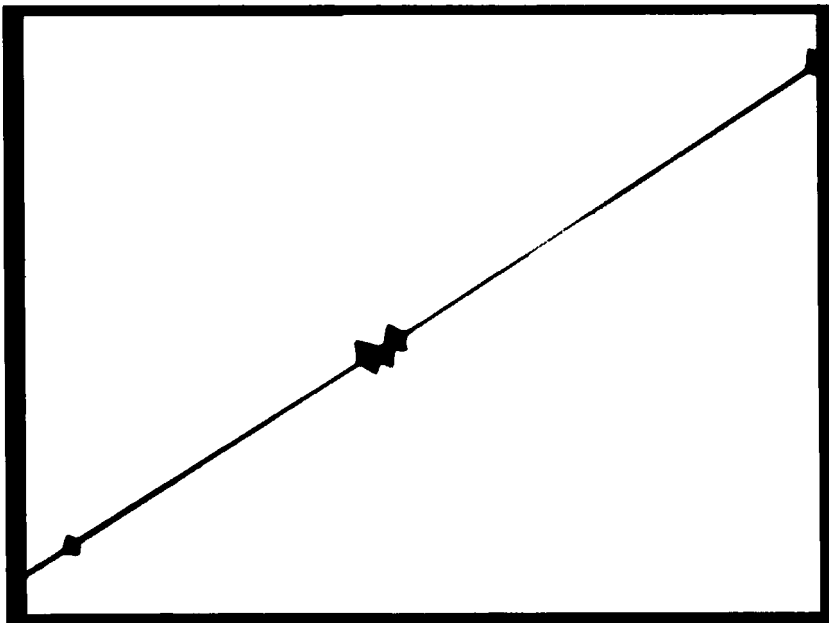


FIGURE 8 Matrix Cracks Formed as a Result of Fragmentation of a $7\ \mu\text{m}$ Diameter Carbon Fiber Embedded in Thermoset Resin. Global Load Applied to the Single Fiber Tension Test Coupon was Transferred to the Fiber *via* Interfacial Shear Stress.

RESULTS AND DISCUSSION

The experimental data are summarily tabulated in Tables II and III. It should be noted that the measured global E , σ_m values and the calculated global σ_m^2/E values obtained with electric heat postcure are not expected to match closely the corresponding values obtained with thermal convective postcure, since thermal gradients exist in specimens heated centrally *via* the carbon fibers while the specimens heated by a convective oven are expected to have uniform temperature distribution within the specimens.

TABLE II
Results of electric resistive heating
(Average data ± 1 root-mean square deviation)

No.	Break number		Crack number*		Modulus		Maximum stress		σ_m^2/E KJ/M ³
	N		N		N	E MPa	N	σ_m MPa	
0	4	66.0 \pm 4.8	4	18.8 \pm 11.2	8	457.9 \pm 68.1	8	9.2 \pm 0.8	186.7 \pm 15.4
1	2	84.0 \pm 7.0	2	27.0 \pm 10.0	4	638.8 \pm 59.1	4	11.9 \pm 0.7	223.4 \pm 33.2
2	2	71.5 \pm 2.5	2	2.5 \pm 0.5	4	747.8 \pm 58.1	4	14.2 \pm 1.2	272.1 \pm 46.8
3	2	76.0 \pm 2.0	2	9.5 \pm 3.5	4	929.0 \pm 94.0	4	17.4 \pm 1.6	327.3 \pm 30.3
4	2	73.0 \pm 3.0	2	4.5 \pm 4.5	4	750.3 \pm 144.5	4	14.3 \pm 1.0	279.1 \pm 34.6
5	2	72.5 \pm 3.5	2	6.0 \pm 3.0	4	918.8 \pm 114.0	4	16.4 \pm 0.6	296.1 \pm 25.5
6	2	73.0 \pm 1.0	2	2.0 \pm 2.0	4	877.8 \pm 142.0	4	16.4 \pm 2.8	305.6 \pm 54.1
7	2	61.0 \pm 1.0	2	0.0 \pm 0.0	4	797.8 \pm 27.9	4	15.5 \pm 1.0	302.5 \pm 34.0
8	2	66.5 \pm 4.5	2	0.0 \pm 0.0	4	860.3 \pm 78.5	4	16.9 \pm 1.4	331.8 \pm 28.0
9	2	64.5 \pm 7.5	2	23.0 \pm 23.0	4	933.5 \pm 120.8	4	17.2 \pm 1.2	320.5 \pm 35.9

(*Cracks with length $a \leq 5\mu\text{m}$ were not counted)

Note:

No. = postcure condition number.

N = number of samples.

TABLE III
Results of convective thermal postcure
(Average data ± 1 root-mean square deviation)

No.	Break number		Crack number*		Modulus		Maximum stress		σ_m^2/E KJ/M ³
	N		N		N	E MPa	N	σ_m MPa	
0	4	66.0 \pm 4.8	4	18.8 \pm 11.2	8	457.9 \pm 68.1	8	9.2 \pm 0.8	186.7 \pm 15.4
1	2	72.5 \pm 4.5	2	10.0 \pm 0.0	4	514.5 \pm 34.5	4	9.9 \pm 0.5	192.6 \pm 29.1
2	2	70.0 \pm 3.0	2	12.0 \pm 6.0	3	542.3 \pm 75.1	4	10.9 \pm 2.3	172.5 \pm 13.1
3	2	65.5 \pm 2.5	2	11.5 \pm 5.5	4	696.3 \pm 95.2	4	12.3 \pm 1.5	219.4 \pm 32.6
4	2	67.5 \pm 0.5	2	5.0 \pm 1.0	4	600.3 \pm 79.4	4	11.7 \pm 0.8	231.7 \pm 33.1
5	2	72.5 \pm 2.5	2	4.5 \pm 2.5	4	811.3 \pm 149.9	3	16.6 \pm 2.3	317.6 \pm 38.0
6	2	72.5 \pm 5.5	2	5.0 \pm 5.0	4	911.0 \pm 78.0	4	18.7 \pm 1.0	382.8 \pm 12.4
7	2	73.5 \pm 3.5	2	5.0 \pm 3.0	4	773.0 \pm 18.9	4	14.2 \pm 0.4	260.5 \pm 12.8
8	2	85.0 \pm 18.0	2	10.5 \pm 10.5	4	888.3 \pm 118.0	4	17.0 \pm 1.2	327.6 \pm 20.3
9	2	78.5 \pm 2.5	2	3.0 \pm 3.0	4	984.3 \pm 64.3	4	17.8 \pm 1.1	320.1 \pm 20.9

(*Cracks with length $a \leq 5\mu\text{m}$ were not counted)

Note:

No. = postcure condition number.

N = number of samples.

The following paragraphs present the discussion of these results to interpret the improvements obtained in fiber-matrix adhesion, matrix (interphase) material properties (E , σ_m , σ_m^2/E) and the fracture behavior of the matrix at the interphase region.

Adhesion

Figure 9 reveals that the application of 3.5 mA of electric heating current increases the numbers of carbon fiber fragments observed in the 50 mm gauge length of specimens, in comparison with specimens for which no electric postcure was applied. Application of higher currents does not produce an additional advantage in reducing the critical fiber length, l_c (which is inversely proportional to the break number) and, in fact, seem to result in longer l_c values with $I = 6.5$ mA. Application of such high amperage may cause the break number to decrease due to forming of highly deformable and/or weak interphase.^{2,3} Note that the average value for the fiber critical length (l_c) can be defined as $l_c = 50 \text{ mm}/(\text{number of carbon fiber breaks})$. Thus, larger break number mean shorter l_c and better adhesion.^{9,10,11} Evaluation of indi-

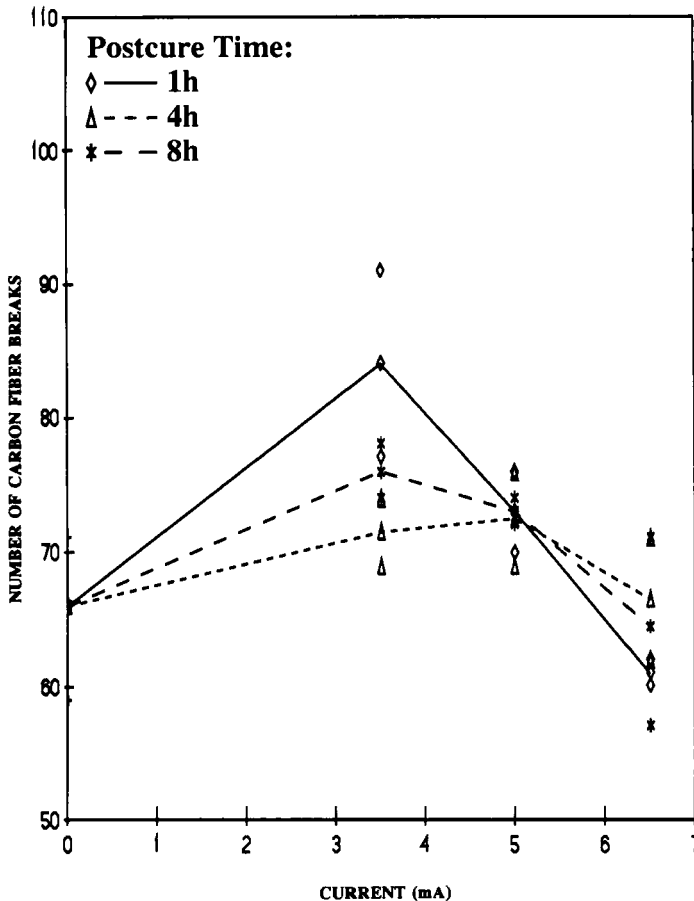


FIGURE 9 Number of Fiber Breaks vs. Fiber Current.

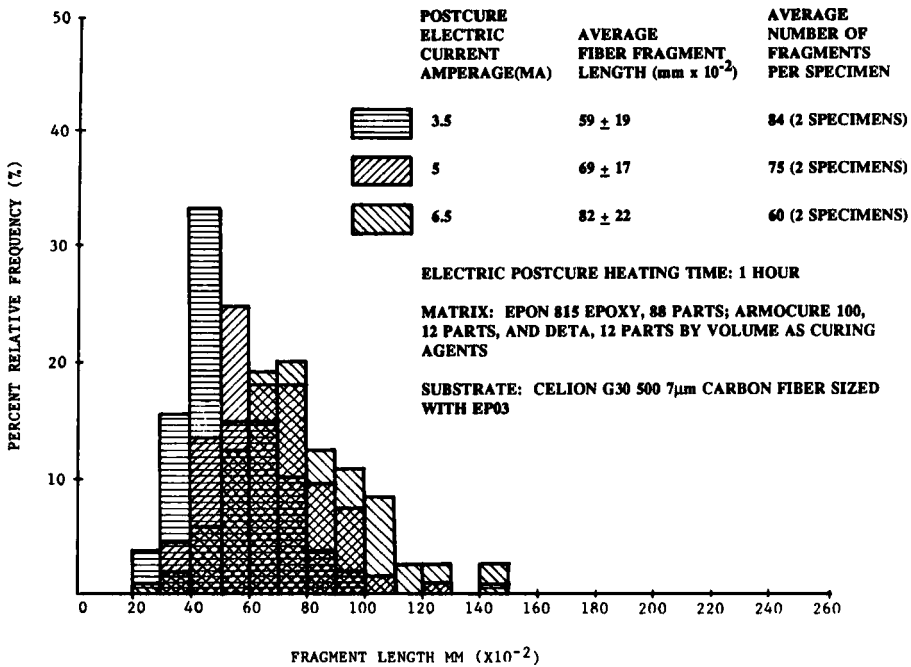


FIGURE 10 The Effect of Postcure Electric Current Amperage Through the Fiber on Fiber-Matrix Adhesion as Indicated by Fragment Size Distribution in Single Fiber Tension Test Specimens Postcured for 1 Hour.

vidual fiber lengths under the microscope and calculation of actual population averages for the critical fiber length values shown in Figure 10 confirmed the results depicted in Figure 9. The shortest average l_c value was calculated as $l_c = (59 \pm 19) \times 10^{-2}$ mm corresponding to one hour application of 3.5 mA and the longest value was $l_c = (82 \pm 22) \times 10^{-2}$ mm corresponding to one hour application of 6.5 mA. Application of 3.5 mA or 5 mA for four hours both resulted in the same average l_c value of $(69 \pm 18) \times 10^{-2}$ mm.

Figure 11 reveals an approximately monotonic increase in the number of fiber fragments with increasing thermal postcure temperature. This postcure procedure, of course, does not produce the severe thermal gradients produced with electric heat postcuring (see the Theory section). It seems that the thermal postcure for 4 hours at higher temperature has some advantage in increasing adhesion over postcuring for 1 or 8 hours at the same temperature (Figure 12). In fact, the shortest l_c value obtained under thermal postcure conditions was $(58 \pm 20) \times 10^{-2}$ mm corresponding to four hours of thermal postcure at 74°C (Figure 12). The longest l_c value was $(72 \pm 16) \times 10^{-2}$ mm corresponding to eight hours of thermal postcure at 39°C.

The reader should note that in Figures 10 and 12 the test conditions which result in the lowest average (mean) fragment length values generally result in the highest frequency bars, corresponding to shorter fragments on the lefthand side of the diagrams, irrespective of their standard deviation values.

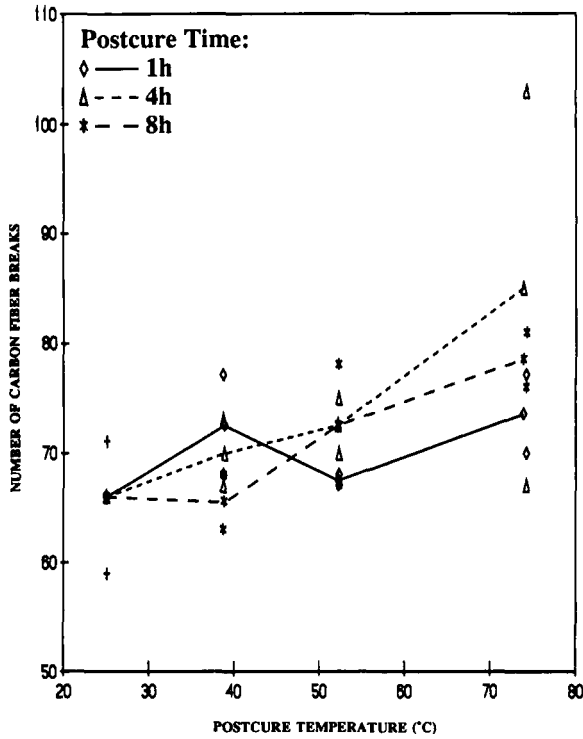


FIGURE 11 Number of Fiber Breaks vs. Convective Thermal Postcure Temperature.

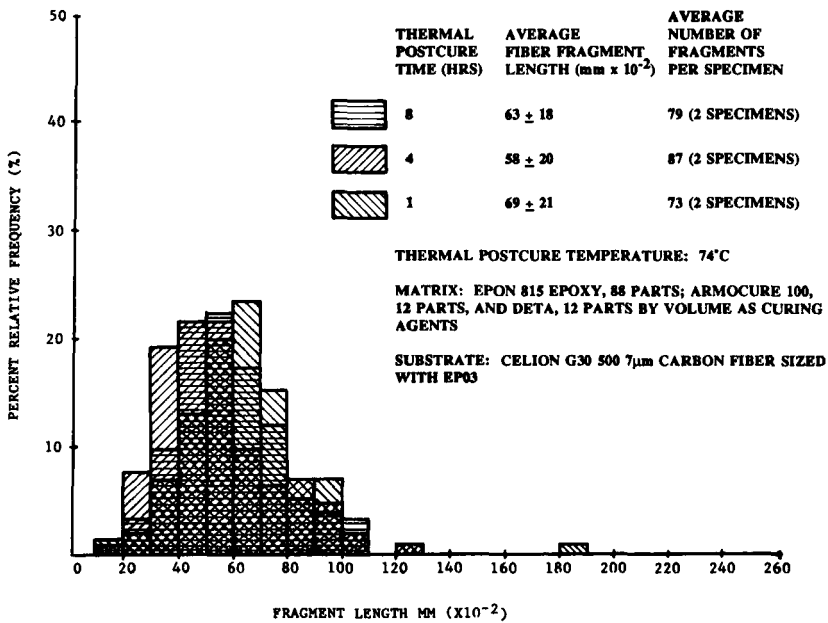


FIGURE 12 The Effect of Convective Thermal Postcure Time on Fiber-Matrix Adhesion as Indicated by Fragment Size Distribution in Single Fiber Tension Test Specimens Postcured at 74°C.

Downloaded At: 14:08 22 January 2011

Modulus of Epoxy Matrix

Examination of Tables II and III reveal that, in general, the elastic modulus of the matrix increases with increasing current or thermal postcure temperatures. The increases in the polymer's elastic modulus resulting from the applied postcure procedures are attributed to increased cross-linking in the thermosetting resin.

Maximum Stress of Epoxy Matrix

The maximum stress is defined as the first global maximum value reached prior to plastic flow in a tensile test of the specimen and it represents the yield stress of the epoxy matrix. As can be observed in Tables II and III, in general, the maximum stress increases with heating current or thermal postcure temperatures. The increases in the polymer's yield stress resulting from the applied postcure procedures are attributed to increased cross-linking and reduction of residual stresses in the thermosetting resin.

The variations in the measured material properties E and σ_m corresponding to the same processing and test conditions are mainly attributed to the presence of impurities and voids within the specimens and to the variations in the epoxy microstructure.

The σ_m^2/E Value

This value is (approximately) related to the G_c or the material toughness. Figure 13 shows that the toughness increases with increased current heating. For 8 hours of heating, it first reaches a maximum in the test parameter range, then decreases. For 1 and 4 hours of electric heating, however, the toughness seems to increase monotonically up to 6.5 mA of current applied. Such higher values of σ_m^2/E mean better toughness. A similar behavior for the toughness is obtained in the thermal postcure (Table III).

Cracks

In Figure 14, with some exceptions, increasing current or temperature decreases the number of cracks observed within the 50 mm gage length of specimens subjected to tensile tests. Thus, it is shown that matrix crack propagation at the fiber fragment ends is less likely with electric current postcured specimens. It is also shown that long time-large current heating does not decrease the number of cracks much further and, in fact, may increase them (8 hours, 6.5 mA current heating, for instance), perhaps due to the forming of a weak interphase at extreme postcure conditions which are likely to decrease the polymer material properties^{3,4} such as strength and modulus. For $I=6.5$ mA with heating time of 1 or 4 hours, however, the number of cracks decreases to zero. One possible reason for this improvement is that the temperature gradient produced by electric heating creates a tougher interphase near the fiber surface as demonstrated in Figure 13 and, consequently, the cracks are unable to propagate easily.

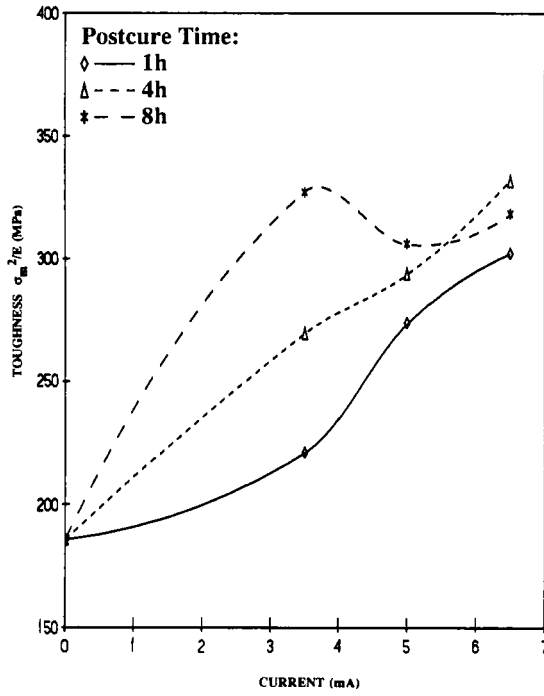


FIGURE 13 σ_m^2/E vs. Fiber Current.

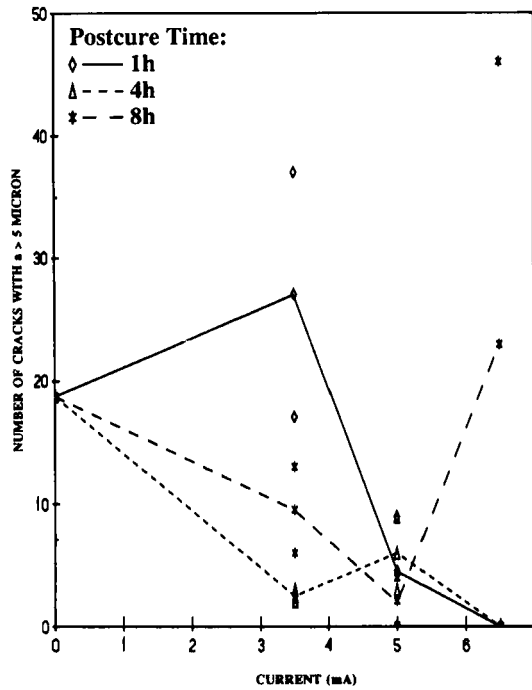


FIGURE 14 Number of Matrix Cracks vs. Fiber Current.

Downloaded At: 14:08 22 January 2011

A similar behavior is obtained when the single-fiber specimens are heated with thermal postcure (Figure 15). Again, the number of matrix cracks decreases with increased thermal postcure temperatures. The reduction in the number of cracks in this case, however, is not as great as that with electric heating at corresponding thermal postcure temperatures. Obviously, the high temperature gradients obtained with electric heating affect the interphase region more efficiently than thermal postcure procedures.

Examination of Table IV reveals that, in general, not only the number but also the size of cracks are smaller with electric postcure when compared with thermal postcure.

The variations in the measured numbers of cracks and fragments corresponding to the same processing and test conditions are attributed to the presence of impurities and voids within the specimens and the variations in the epoxy microstructure.

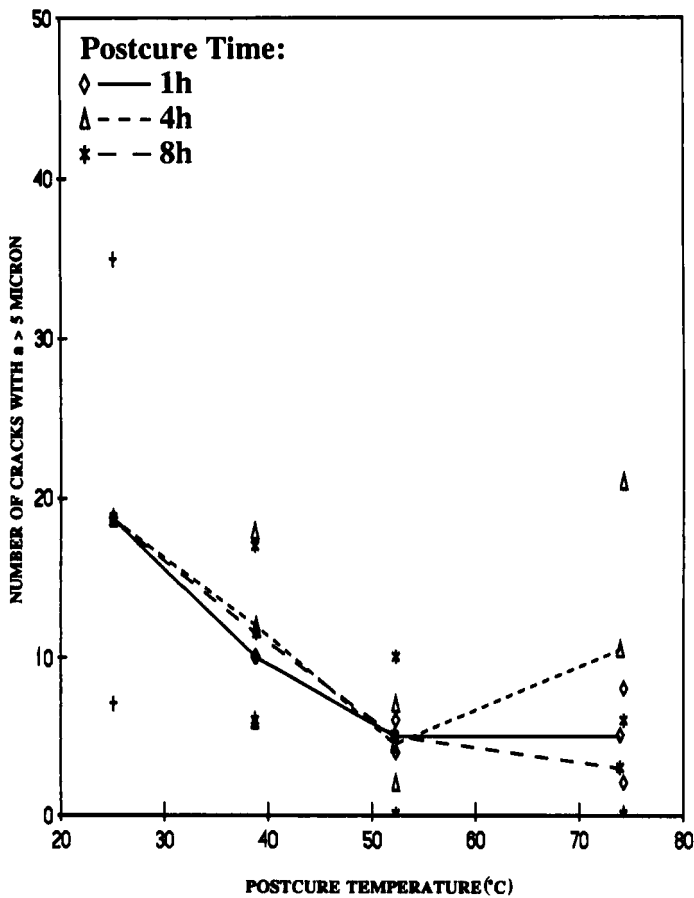


FIGURE 15 Number of Matrix Cracks vs. Convective Thermal Postcure Temperature.

TABLE IV
The classification of the maximum cracks

No.	Postcure type	$a \leq 5\mu\text{m}$	$5\mu\text{m} < a \leq 20\mu\text{m}$	$20\mu\text{m} < a \leq 40\mu\text{m}$	$40\mu\text{m} < a \leq 60\mu\text{m}$	$a > 60\mu\text{m}$	N
0				2	1	1	4
1	Electric heating			2			2
2	Electric heating			2			2
3	Electric heating		2				2
4	Electric heating	1				1	2
5	Electric heating		2				2
6	Electric heating	1	1				2
7	Electric heating	2					2
8	Electric heating	2					2
9	Electric heating	1	1				2
1	Thermal postcure		2				2
2	Thermal postcure		2				2
3	Thermal postcure		1	1			2
4	Thermal postcure		1	1			2
5	Thermal postcure		1	1			2
6	Thermal postcure	1		1			2
7	Thermal postcure				1	1	2
8	Thermal postcure	1		1			2
9	Thermal postcure	1	1				2

Note:

No. = postcure condition number.

N = number of samples.

DISCUSSION

The experimental results revealed that the elastic modulus, maximum stress and toughness (σ_m^2/E) of the matrix behave similarly. They increase as a result of postcure by electric heating or thermal heating which increases the cross-link density of the epoxy resin and reduces the residual stresses. The benefits of postcure, however, are limited by the amounts of fiber current, temperature and postcure time that can be applied before the material properties of the matrix are deteriorated due to microstructural changes. For example, at high temperature (above T_g , the glass transition temperature), the oxidation and degradation will increase quickly thus deteriorating the material properties of the matrix.^{13,27} Crack initiation and propagation are intimately related to σ_m^2/E and, consequently, to the maximum stress and elastic modulus of the epoxy resin. The investigation illustrates that by using electric heating it is possible to increase σ_m^2/E and maximum stress properties for the fiber-matrix interphase and, consequently, reduce the number and size of cracks resulting from fiber fragmentation.

CONCLUSIONS

It seems that resistive electric heating of the single carbon fiber can provide information about the effects of the temperature gradients on the carbon-epoxy interphase.

Based on the experimental data the following conclusions can be made:

- It is possible to use electric heating to improve the material properties of carbon fiber-epoxy matrix composites for increasing the interfacial adhesion and preventing the initiation and propagation of cracks in the epoxy matrix.
- Electric heating of the cured thermoset composite *via* the carbon fiber serves to postcure it.
- The benefits obtained by this postcure procedure are similar to those obtained by convective thermal postcure of the specimens except that the heat is applied at the interphase to tailor its properties and the temperature gradients produced are much higher with resistive electric heating.
- Resistive electric postcuring is a more efficient process, since less energy is used and it is placed directly where it is needed.
- The postcure procedures applied affect the elastic modulus, maximum stress and toughness of the matrix similarly, with these properties increasing up to a limit with increased energy input. Further energy input results in deterioration of these properties due to microstructural changes.

Consequently, better understanding of the interphase microstructure is necessary for efficient application of cure and postcure processes such as resistive electric heating. Research into large scale industrial application of resistive electric heating of carbon supported composite structures is also necessary for this process to become a practical industrial procedure.

Acknowledgements

Financial support from the Grumman Corporation is gratefully acknowledged. We also would like to thank Dr. S. W. Yurgartis for his suggestions and Dr. A. Turgut for his help in processing the fiber fragment data.

References

1. R. Agrawal and L. T. Drzal, *J. Adhesion* **29**, 63 (1989).
2. E. Sancaktar and P. Zhang, *J. Mech. Design* **112**, 605 (1990).
3. E. Sancaktar, H. Jozavi and R. M. Klein, *J. Adhesion* **15**, 241 (1983).
4. H. Jozavi and E. Sancaktar, *J. Adhesion* **18**, 25 (1985).
5. H. Jozavi and E. Sancaktar, *J. Adhesion* **27**, 143 (1989).
6. D. Broek, *Elementary Engineering Fracture Mechanics* (Martinus Nijhoff Publishers, Boston, 1983).
7. K. Hellan, *Introduction to Fracture Mechanics* (McGraw-Hill Inc., New York, 1984).
8. D. K. Felbeck and A. G. Atkins, *Strength and Fracture of Engineering Solids* (Prentice Hall Inc., Englewood Cliffs, New Jersey, 1984).
9. L. T. Drzal, M. J. Rich and P. F. Lloyd, *J. Adhesion* **16**, 1 (1982).
10. L. T. Drzal, M. J. Rich and M. F. Koenig, *J. Adhesion* **18**, 49 (1985).
11. W. D. Bascom and R. M. Jensen, *J. Adhesion* **19**, 219 (1986).
12. H. Lee and K. Neville, *Handbook of Epoxy Resins* (McGraw-Hill Inc., New York, 1967).
13. H. F. Mark, N. M. Bikales, C. G. Overberger and G. Menges, *Encyclopedia of Polymer Science and Engineering*, Vol. 6, 2nd ed. (John Wiley and Sons, New York, 1985).
14. D. J. Alner, *Aspects of Adhesion* (University of London Press Ltd, 1969).
15. A. C. Loos and G. S. Springer, *J. Composite Materials* **17**, 135 (1983).
16. R. O. Ebewele, B. H. River and J. A. Koutsky, *J. Adhesion* **14**, 189 (1982).

17. J. Muzzy, L. Norpoth and B. Varughese, *SAMPE J.* **25**, 23 (1989).
18. P. H. Dara and A. C. Loos, NASA Interim Report 57, VPI&SU, Sept. 1985.
19. A. Kelly and W. R. Tyson, *Mech. Phys. Solids* **13**, 329 (1965).
20. L. Dilandro, A. T. Dibenedetto and J. Groeger, *Polymer Composites* **9**, 209 (1988).
21. W. D. Bascom, R. L. Cottingham and C. O. Timmons, *J. App. Poly. Sci.: Applied Polymer Symposia* **32**, 165 (1977).
22. S. W. Tsai and H. T. Hahn, in *Polymer Science and Technology Series 12-B, Adhesion and Adsorption of Polymers*, L. H. Lee, Ed. (Plenum Press, New York, 1980), p. 463.
23. D. L. Hunston, A. J. Kinloch, S. J. Shaw and S. S. Wang, in *Adhesive Joints*, K. L. Mittal, Ed. (Plenum Press, New York, 1984), p. 789.
24. E. Sancaktar, J. Baldwin and J. Tang, *J. Adhesion*, **23**, 233 (1987).
25. M. R. Piggott and P. S. Chua, in *Composites and Other New Materials for PVP: Design and Analysis Considerations*, PVP, Vol. 174, G. E. O. Widera, Ed. (ASME, New York, 1988), p. 143.
26. G. H. Golub and C. F. Van Loan, *Matrix Computation* (John Hopkins University Press, Baltimore, 1989).
27. J. B. Enns and J. K. Gillham, *J. App. Poly. Sci.* **28**, 2587 (1983).